Available online at www.sciencedirect.com

ScienceDirect

Journal of Catalysis 254 (2008) 238–243

JOURNAL OF CATALYSIS

www.elsevier.com/locate/jcat

On the usefulness of carbon isotopic exchange for the operando analysis of metal–carbonyl bands by IR over ceria-containing catalysts

H. Daly [a], J. Ni [a], D. Thompsett [b], F.C. Meunier [a,c,*]

[a] *CenTACat, School of Chemistry and Chemical Engineering, Queen's University, Belfast, BT9 5AG, UK*
[b] *Johnson Matthey Technology Centre, Blounts Court, Sonning Common, Reading, RG4 9NH, UK*
[c] *Laboratoire Catalyse et Spectrochimie, CNRS, University of Caen, ENSICAEN, 6 Boulevard du Marechal Juin, 14050 Caen Cedex, France*

Received 12 October 2007; revised 19 December 2007; accepted 25 December 2007

Abstract

Operando diffuse reflectance FTIR spectroscopy (DRIFTS) combined with isotopic exchange techniques were used to investigate the bands located in the carbonyl-stretching region observed over a Au/$CeZrO_4$ catalyst under water–gas shift (WGS) conditions. The use of ^{12}CO and ^{13}CO in the feed was essential to distinguish between Au-carbonyl bands and an electronic transition band associated with Ce^{III} centers and to allow correct deconvolution of the carbonyl signal. The very active WGS catalyst used here as an example displays three main types of carbonyl species under reaction conditions, tentatively assigned to CO adsorbed on positively charged, neutral, and negatively charged Au entities. The DRIFTS data collected in the present work characterize the catalyst under reaction conditions and thus circumvent the difficulties associated with possible catalyst modifications during and after use. The possible presence of the electronic absorption (the maximum of which is at ca. 2120–2140 cm^{-1}) due to the presence of Ce^{III} centers always should be considered when analyzing metal–carbonyl IR bands. It also is crucial to realize that this band also may form in situ by reduction of the Ce^{IV} while under reaction conditions or when the sample is titrated with CO.

Keywords: FTIR; DRIFTS; In situ; Operando; Isotope; Exchange; SSITKA; Carbonyl; Ceria; Metal; Gold

1. Introduction

Catalysts based on ceria-supported metals (e.g., Cu, Pt, Au) display high activity for various reactions involving carbon monoxide, such as CO oxidation [1–4], the preferential oxidation of CO in the presence of hydrogen (PROX) [5–8], and the water–gas shift (WGS) reaction [9–17]. The adsorption of CO over the metal to form a metal carbonyl species is usually taken to be the first reaction step. Therefore, understanding the features of the metal–CO bond is valuable. This can be achieved by, for instance, analyzing the intensity and wavenumber of the carbonyl bands that are observable by IR spectroscopy. Such data may help in determining the nature (neutral or electronically charged) of the metal particles, the dispersion of the metallic phase, the type of bonding (e.g., on-top, bridged carbonyl), and the presence of lateral interactions between adsorbates.

Gold supported on ceria-containing supports has received particular attention in recent years in view of the high activity at low temperatures for the above-mentioned reactions that some appropriately prepared formulations can exhibit [18,19]. There has been much debate as to the nature of the active gold species, with the activity being related to various factors, including the size and shape of the metal particles, the nature of the support, and its electronic interaction with the metallic phase and the metal oxidation state [20,21]. Work by Boccuzzi et al. [22–27] and Hadjiivanov et al. [28–32] have provided some valuable insight into the state of Au particles by analyzing IR carbonyl bands.

Much of the previous work on the characterization of Au and Ce-based catalysts through metal carbonyl bands was not carried out under reaction conditions (operando), but rather was done using in situ methods, such as measures under dynamic vacuum after exposure to gas-phase CO or under varying pressures of pure CO. Operando techniques are invaluable for providing information on a working catalyst, because the structure

---

[*] Corresponding author. Fax: +33 (0) 231452822.
E-mail address: frederic.meunier@ensicaen.fr (F.C. Meunier).

0021-9517/$ – see front matter
doi:10.1016/j.jcat.2007.12.013

of the Au particles and the oxidation state of the metal (and also that of the cerium atoms of the support) can evolve under reaction conditions. As an example, operando EXAFS and XANES of the Au/$CeZrO_4$ catalyst that we investigated in the present work revealed that the sample contained oxidized gold at room temperature in air, whereas only metallic gold could be observed at 100 °C under a WGS feed [33]. Similar results on Au and ceria-based catalysts were reported by Hanson et al. [34].

The extent of the catalyst modification under reaction conditions is not easily predictable and also will depend on the interaction between Au and the support. It has been shown that gold can significantly reduce the reduction temperature of ceria by several hundreds of degrees and that ceria surface reduction can be seen at temperatures as low as 100 °C [18,23]. The reducing nature of CO-containing atmospheres such as WGS feeds usually will lead to the formation of reduced species of cerium, at least on the catalyst surface [18,35–37]. This even occur even in the presence of $CO + O_2$ feeds with a large excess of O_2, because at low temperatures, the oxidation state of the surface under steady-state reaction conditions will be dictated primarily by the kinetics of the sample reduction by CO versus that of oxidation by O_2, rather than by the thermodynamics of the overall system.

The reduction of Ce^{IV} to Ce^{III} leads to additional difficulties in the interpretation of metal carbonyl bands. Reduced ceria exhibits an absorption band in the infrared region at approximately 2120 cm^{-1} due to a normally forbidden electronic transition ($^2F_{5/2}$ to $^2F_{7/2}$) [38–42]. Binet et al. observed this band after H_2 or $^{12}CO/^{13}CO$ reduction of ceria. The band wavenumber did not shift regardless of whether treatment was carried out with ^{12}CO or ^{13}CO, demonstrating that the band is not due to any carbonyl species. Depending on the baseline correction method used, the position of the maximum of this band can (apparently) shift within the 2140–2120 cm^{-1} wavenumber range [42]. The presence of this electronic absorption band located in the same region as that associated with typical carbonyl-stretching modes may lead to misinterpretation of data even at very low temperatures, because metals such as Au lower the reduction temperature at the surface of ceria.

An example of the difficulty created by this electronic transition was recently provided by Behm et al. [43], who acknowledged the difficulty in interpreting the IR signal in the 2200–2000 cm^{-1} region (see their Fig. 5b). A possible explanation for this proposed by Behm et al. assigns most of the signal in this region to the electronic transition of reduced ceria. We favor this interpretation over a second possibility proposed by Behm et al. that this band is due to carbonyl species adsorbed on Au(0). The latter interpretation led to the unrealistic conclusion that "the constant CO(ads) intensity is most simply explained by a compensation of two counteracting effects, deactivation (intensity decrease) and formation of Au(0) nanoparticles (intensity increase)," [43] when trying to explain the fact that no signal change occurred while the surface state of gold was dramatically modified. The difficulty of rationalizing the IR signal in this region clearly supports the need for the work described in this report.

The combination of IR spectroscopy and steady-state isotopic transient kinetic analysis (SSITKA [44]) provides a powerful method for investigating the reactivity of surface species under reaction conditions [45–48]. Using SSITKA-DRIFTS-MS methods, we were able to prove that the IR-observable surface formates are not important factors in the WGS reaction mechanism for various catalysts: Au/$CeZrO_4$ [49], Pt/ZrO_2 [50], Au/Ce(La)O_2 [42], and Pt/CeO_2 [49,51]. Our findings underscore an additional advantage of using such a technique: the ability to monitor the structure of the metal carbonyl band under reaction conditions and ascertain deconvolution of the signal by comparing the data obtained under ^{12}C- and ^{13}C-containing feeds. The discrimination between the signal of metal carbonyl species and that of the reduced ceria electronic transition is made obvious, allowing straightforward spectrum corrections. The WGS data used in the present work were collected by operando DRIFTS over a Au/$CeZrO_4$ catalyst, which is among the most active low-temperature WGS catalyst based on noble metals reported so far [19,33,52].

2. Experimental

The experimental setup consisted of a high-temperature diffuse reflectance IR cell (from Spectra-Tech) fitted with ZnSe windows. The DRIFTS cell was located in a Bruker Equinox 55 spectrometer, operating at a resolution of 4 cm^{-1}. The reactor crucible was modified to ensure plug-flow conditions throughout the catalyst bed. The interface between the ceramic reactor and the metallic base plate was sealed with PTFE tape to prevent any sample bypass. The original porous bed for supporting the sample was replaced by an inert metallic mesh. The WGS reaction rates measured with this cell were equal to those measured in a conventional tubular plug-flow reactor [42].

The catalyst used was a 2 wt% Au/$CeZrO_4$, the details of which have been reported previously [33]. The catalyst sample of 60 ± 3 mg was placed in the crucible. The purity of all gases used (i.e., H_2, CO, Ar; all supplied by BOC) was >99.95%. The ^{13}CO (supplied by Cambridge Isotope Laboratories Inc.) was 99% pure. The DRIFTS cell was connected to the feed gas cylinders through low-volume stainless-steel lines. The gas flows were controlled by Aera mass flow controllers, which were calibrated regularly. A 4-way valve was used to allow rapid switching between two reaction feeds when appropriate. High-purity water was introduced using a single saturator that delivered a constant, accurate flow of water. Water delivery was completely unaffected by the valve switching (as determined by MS or GC analyses [51]).

A reference DRIFTS single scan was recorded over a mirror at room temperature and used as background; 28 and 128 scans were co-added for the sample and background spectra, respectively. Unless stated otherwise, the catalyst was brought up to reaction temperature under Ar, after which water was added to the Ar stream. The reaction mixture was subsequently introduced at a total flow rate of 100 mL min^{-1}. The reaction flow was down through the reactor bed; therefore, the upper layer of the catalyst (the layer mainly probed by the DRIFTS technique) was the front of the bed. Steady-state conditions in terms of the

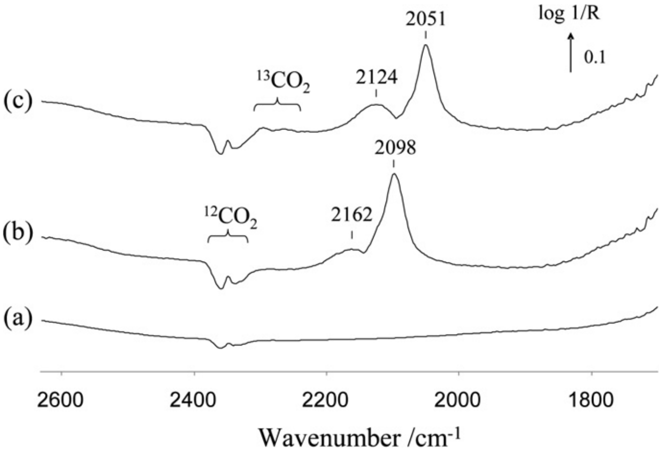

Fig. 1. In situ DRIFTS spectrum of the Au/CeZrO$_4$ at steady-state under (a) a stream of Ar, (b) a stream of 2.5% ^{12}CO + 7% H_2O + 13% H_2 in Ar and (c) the same feed as (b) but with ^{13}CO in place of ^{12}CO. $T = 125\,^\circ$C. The contribution of gas-phase CO is present.

concentration of the surface species measured by DRIFTS were reached in less than 30 min. The IR data are reported as $\log 1/R$, with $R = I/I_0$, where R is the sample reflectance, I_0 is the intensity measured on the sample after exposure to the CO-free feed, and I is the intensity measured under reaction condition. The pseudo-absorbance $\log 1/R$ gave a better linear representation of the band intensity against sample surface coverage than that given by the Kubelka–Munk function for strongly absorbing media, such as those based on CeO$_2$ [53].

3. Results and discussion

The typical in situ DRIFT spectrum obtained during the WGS reaction at 125 °C over the highly active Au/CeZrO$_4$ has been described in detail elsewhere [49,52]; only the region relevant to carbonyl vibration is discussed here. No band was observed under Ar at the reaction temperature over the catalyst in the 2600–2200 cm^{-1} region, except for those of atmospheric CO$_2$ at 2400–2300 cm^{-1} (Fig. 1a). A major carbonyl band at 2097 cm^{-1} was observed under a nonlabeled WGS feed, 2.5% ^{12}CO + 7% H_2O + 13% H_2 in Ar (Fig. 1b). The carbonyl absorbing at this wavenumber has been proposed to be that adsorbed on the edge and/or defect sites of metallic gold particles [1,22–26,28–32]. Another band at 2162 cm^{-1} and a shoulder on the high-wavenumber side of the main carbonyl peak also were seen, due mainly to absorption by gas-phase CO [54].

The ^{12}CO of the feed was then replaced with ^{13}CO, keeping the overall chemical composition of the feed identical, 2.5% ^{13}CO + 7% H_2O + 13% H_2 in Ar. The carbonyl exchange over this catalyst was completed in about 6 s (data not shown) and resulted in the main DRIFTS band shifting from 2098 down to 2051 cm^{-1} (Fig. 1c), the value expected based on the increase in the reduced mass of the CO vibrator [wavenumber ratio = (reduced mass ratio)$^{0.5}$ = 1.023]. The duration of the carbonyl exchange was equal to that of the exchange of CO(g) and of the Kr tracer (not shown). This observation indicates that the exchange time of these species was limited by the purging of the system, and thus no intrinsic kinetic information on the reactivity of carbonyl can be extracted from these data. (This would require a system with a much lower dead volume.) The second main band observed was due to the absorption of ^{13}CO at 2124 cm^{-1} (Fig. 1c). Other bands at 2300–2200 cm^{-1} were due to the reaction product $^{13}CO_2$.

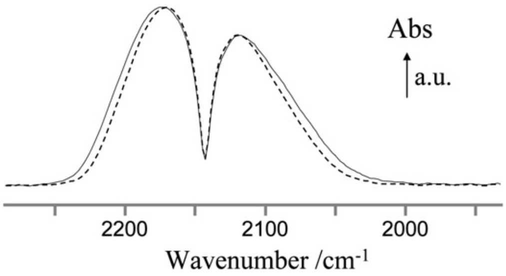

Fig. 2. In situ DRIFTS spectrum of 1% ^{12}CO in Ar measured over a KBr sample at 35 °C (dashed line) and at $T = 125\,^\circ$C (solid line). The same KBr sample under Ar was used as background. The spectrum intensities were normalized to allow directly comparing the spectral width.

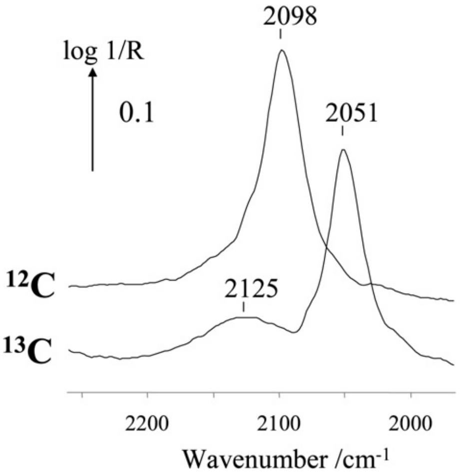

Fig. 3. In situ DRIFTS spectrum collected over the Au/CeZrO$_4$ at steady-state under a stream of 2.5% ^{12}CO + 7% H_2O + 13% H_2 in Ar (top curve) and the same feed but with ^{13}CO in place of ^{12}CO (bottom curve). $T = 125\,^\circ$C. The contribution of gas-phase CO was subtracted.

The contribution of gas-phase CO had to be subtracted to deconvolute the carbonyl signal properly. This necessitated using ^{12}CO and ^{13}CO spectra recorded at the same reaction temperature (i.e., 125 °C), because a spectrum collected at a different temperature (e.g., room temperature) would have a different distribution of rotational states and thus a different band shape. This is exemplified by the ^{12}CO spectra measured over a KBr sample at 35 and 125 °C in our DRIFTS cell (Fig. 2); although the difference between the temperatures at which the two CO spectra were recorded was <100 °C, the bandwidths were significantly different.

The spectra obtained after subtraction of the CO gas-phase contribution are shown in Fig. 3 (with a baseline offset) and Fig. 4 (with no baseline offset). Interestingly, the spectrum obtained under the labeled feed exhibited a well-resolved band at ca. 2125 cm^{-1} alongside the main Au–^{13}CO band at 2051 cm^{-1} (Fig. 3, bottom spectrum). This band could not correspond to any ^{13}C-containing carbonyl species; otherwise, a band of sim-

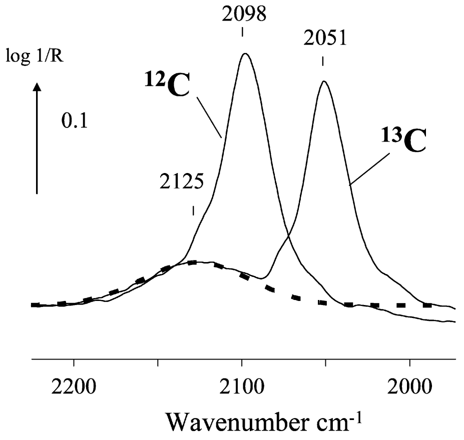

Fig. 4. Same spectra as shown in Fig. 3, with no baseline offset. The dashed line is a Gaussian curve fitting the band associated with the electronic transition of reduced ceria.

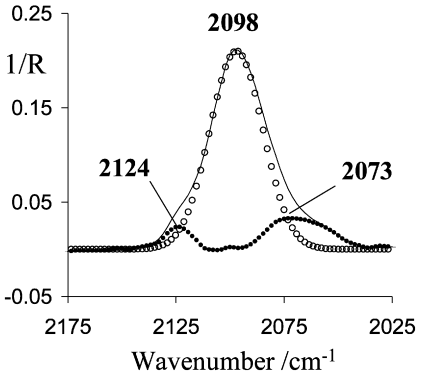

Fig. 5. Deconvolution of the ^{12}C-containing carbonyl DRIFTS bands collected over the 2 wt% Au/$CeZrO_4$ at steady-state under WGS feed. The measured spectrum is represented by a solid line. The main central band was fitted to a Gaussian curve (○). The difference between the measured spectrum and the Gaussian central band is represented by the dotted curve (●). $T = 125\,°C$. Feed: 2.5% ^{12}CO, 7% H_2O, 13% H_2 in Ar. The contribution of gas-phase CO and that of the reduced ceria electronic transition at 2125 cm^{-1} were both subtracted from the raw spectrum.

ilar intensity located at 2175 cm^{-1} in the ^{12}C-related spectrum would be expected, which clearly was not the case (Fig. 3, upper spectrum). Therefore, the band at 2125 cm^{-1}, which was well fitted by a Gaussian curve (Fig. 4, dashed curve), can be assigned to the electronic transition of reduced ceria, as it has been discussed in the case of other ceria-based catalysts as well [38–42]. This observation stresses that a fraction of the cerium atoms of the support were partially reduced (Ce^{IV} to Ce^{III}) under reaction conditions, in contrast to the findings for the fresh material or material exposed to Ar, which are typically used to record the background signal. Because the ceria is partly reduced under reaction conditions (at least on the surface), the support likely will inject electronic density into the metal particle, modifying the CO–metal interaction [55].

The contribution to the spectra from the electronic transition of ceria (which was assimilated to the dashed curve in Fig. 4) was subtracted to allow investigation of the intrinsic structure of the Au-carbonyl bands. The corrected (from both gas-phase CO and Ce^{III} electronic transition) Au-carbonyl spectra corresponding to the ^{12}C and ^{13}C are shown in Figs. 5 and 6 (solid line), respectively. Both spectra were deconvoluted using a Gaussian curve (open circle) to fit the main central band. The difference between the actual spectra and the central Gaussian curves are plotted using full circle symbols in each case. The difference spectra display two bands, one on each side of the main central band. Any further deconvolution of the side bands was not attempted. Clearly, the set of bands obtained for the ^{12}C spectrum (Fig. 5) were essentially identical in shape and intensity to those obtained for the ^{13}C spectrum (Fig. 6). Moreover, the ratio of the shifted band wavenumbers was exactly what was expected (i.e., 1.023) due to the differences in reduced mass between the ^{12}CO and ^{13}CO vibrators: 2124 to 2076 cm^{-1}, 2098 to 2051 cm^{-1}, and 2073 to 2027 cm^{-1}.

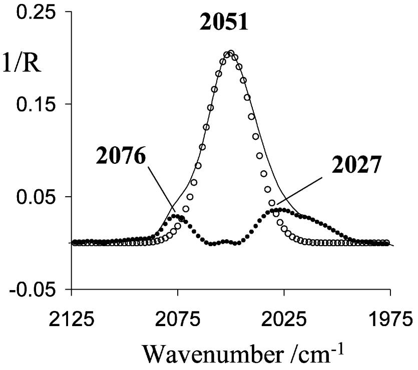

Fig. 6. Deconvolution of the ^{13}C-containing carbonyl DRIFT bands collected over the 2 wt% Au/$CeZrO_4$ at steady-state under WGS feed. The measured spectrum is represented by a solid line. In both cases, the main central band was fitted to a Gaussian curve (○). The difference between the measured spectrum and the Gaussian central band is represented by the dotted curve (●). $T = 125\,°C$. Feed: 2.5% ^{13}CO, 7% H_2O, 13% H_2 in Ar. The contribution of gas-phase CO and that of the reduced ceria electronic transition at 2125 cm^{-1} were both subtracted from the raw spectrum.

The similarity between the ^{12}C- and ^{13}C-carbonyl deconvoluted spectra underscores the high degree of reliability of our data analysis in terms of band nature and location, which would not have been possible using only the ^{12}C data. Note that one of the ^{12}C-containing carbonyls detected in the present study—that associated with the 2124–cm^{-1} band—absorbed at the position of the reduced ceria electronic transition absorption (2125 cm^{-1}) and thus would normally be very difficult to resolve. In a different set of experiments (results not shown), we attempted to correct for the electronic transition data by simply recording background spectra on catalysts prereduced by H_2; however, this led to ambiguous data, because CO also was formed through surface carbonate reduction, and the intensity of the electronic transition band varied with experimental conditions, probably due to varying Ce reduction.

Although the aim of the present work was not to determine the exact nature of the various carbonyls observed on the catalyst, suggesting some tentative assignments is probably sensible. In the ^{12}C-containing carbonyl, as mentioned above, the band around 2100 cm^{-1} has been assigned to CO adsorbed on metallic Au [1,21–30]. The broad band on the low-wavenumber side with an apparent maximum at 2073 cm^{-1} is likely due to adsorption of CO on negatively charged Au atoms or particles, as reported by Bocuzzi et al. for several Au-based systems [22, 25,27]. CO adsorbed on Au^{I+} (as in zeolite-based samples) showed a typical band at 2150 cm^{-1}, and thus the band observed at 2124 cm^{-1} was assigned to CO adsorbed on a Au site with a partial positive charge. These assignments are tentative; more work is needed to unravel the electronic properties of the adsorption sites. Such work would be worthwhile, because the catalyst's activity is linked to its ability to adsorb CO at low temperature [52], which in turn likely depends on the electronic transfer between the support and Au atoms [55].

4. Conclusion

Based on our findings, we can draw the following conclusions from the present study:

1. The use of steady-state isotope transient techniques coupled with DRIFTS analysis allowed us to unambiguously discriminate between the signals of carbonyl species and those arising from absorption bands not related to CO(ads).
2. The DRIFTS data collected in the present work characterize the catalyst under reaction conditions and thus circumvent the difficulties associated with possible catalyst modifications during and after use.
3. The possible presence of electronic absorption (the maximum of which occurred around 2120–2140 cm^{-1}) due to the presence of Ce^{III} centers must be taken into account when analyzing metal–carbonyl IR bands. It is crucial to recognize that such bands also may form in situ through reduction of the Ce^{IV} under reaction conditions or when the sample is titrated with CO.
4. The very active WGS catalyst used here as an example displays three main types of carbonyl species under reaction conditions, tentatively assigned to CO adsorbed on positively charged, neutral, and negatively charged Au entities.

Acknowledgment

This work was partly supported by the EPSRC under the CARMAC Project.

References

[1] G.C. Bond, D.T. Thompson, Catal. Rev. Sci. Eng. 41 (1999) 319.
[2] A.M. Venezia, G. Pantaleo, A. Longo, G. Di Carlo, M.P. Casaletto, F.L. Liotta, G. Deganello, J. Phys. Chem. B 109 (2005) 2821.
[3] D. Gamarra, G. Munuera, A.B. Hungria, M. Fernandez-Garcia, J.C. Conesa, P.A. Midgley, X.Q. Wang XQ, J.C. Hanson, J.A. Rodriguez, A. Martinez-Arias, J. Phys. Chem. C 111 (2007) 11026.
[4] V. Aguilar-Guerrero, B.C. Gates, Chem. Commun. 30 (2007) 3210.
[5] D. Teschner, A. Wootsch, O. Pozdnyakova-Tellinger, J. Kröhnert, E.M. Vass, M. Hävecker, S. Zafeiratos, P. Schnörch, P.C. Jentoft, A. Knop-Gericke, R. Schlögl, J. Catal. 249 (2007) 318.
[6] M. Manzoli, F. Vindigni, A. Chiorino, T. Tabakova, V. Idakiev, F. Boccuzzi, React. Kinet. Catal. Lett. 91 (2007) 213.
[7] G. Avgouropoulos, J. Papavasiliou, T. Tabakova, V. Idakiev, T. Ioannides, Chem. Eng. J. 124 (2006) 41.
[8] W. Deng, M. Flytzani-Stephanopoulos, Angew. Chem. Int. Ed. 45 (2006) 2285.
[9] A. Karpenko, R. Leppelt, J. Cai, V. Plzak, A. Chuvilin, U. Kaiser, R.J. Behm, J. Catal. 250 (2007) 139.
[10] T. Tabakova, V. Idakiev, J. Papavasiliou, G. Avgouropoulos, T. Ioannides, Catal. Commun. 8 (2007) 101.
[11] A. Luengnaruemitchai, S. Osuwan, E. Gulari, Catal. Commun. 4 (2003) 215.
[12] D. Tibiletti, A. Goguet, F.C. Meunier, J.P. Breen, R. Burch, Chem. Commun. (2004) 1636.
[13] Y. Li, Q. Fu, M. Flytzani-Stephanopoulos, Appl. Catal. B Environ. 27 (2000) 179.
[14] H. Sakurai, T. Akita, S. Tsubota, M. Kiuchi, M. Haruta, Appl. Catal. A 291 (2005) 179.
[15] D. Andreeva, V. Idakiev, T. Tabakova, A. Andreev, J. Catal. 158 (1996) 354.
[16] S. Hilaire, X. Wang, T. Luo, R.J. Gorte, J. Wagner, Appl. Catal. A 215 (2001) 271.
[17] R. Leppelt, B. Schumacher, V. Plzak, M. Kinne, R.J. Behm, J. Catal. 244 (2006) 137.
[18] Q. Fu, H. Saltsburg, M. Flytzani-Stephanopoulos, Science 301 (2003) 935.
[19] R. Burch, Phys. Chem. Chem. Phys. 8 (2006) 5483.
[20] M. Haruta, N. Yamada, T. Kobayashi, S. Iijima, J. Catal. 115 (1989) 301.
[21] J.C. Fierro-Gonzalez, B.C. Gates, Catal. Today 122 (2007) 201.
[22] T. Tabakova, F. Boccuzzi, M. Manzoli, J.W Sobczak, V. Idakiev, D. Andreeva, Appl. Catal. B 49 (2004) 73.
[23] T. Tabakova, F.B. Boccuzzi, M. Manzoli, D. Andreeva, Appl. Catal. A 252 (2003) 385.
[24] M. Manzoli, F. Boccuzzi, A. Chiorino, F. Vindigni, W. Deng, M. Flytzani-Stephanopoulos, J. Catal. 245 (2007) 306.
[25] T. Tabakova, F. Boccuzzi, M. Manzoli, J.W. Sobczak, V. Idakiev, D. Andreeva, Appl. Catal. A 298 (2006) 127.
[26] M. Manzoli, F. Boccuzzi, A. Chiorino, F. Vindigni, W. Deng, M. Flytzani-Stephanopoulos, J. Catal. 244 (2006) 137.
[27] F. Menegazzo, M. Manzoli, A. Chiorino, F. Boccuzzi, T. Tabakova, M. Signoretto, F. Pinna, N. Pernicone, J. Catal. 237 (2006) 431.
[28] M.A. Centeno, K. Hadjiivanov, T. Venkov, H. Klimev, J.A. Odriozola, J. Mol. Catal. A 252 (2006) 142.
[29] K. Hadjiivanov, G. Vayssilov, Adv. Catal. 47 (2002) 347.
[30] H. Klimev, K. Fajerwerg, K. Chakarova, L. Delannoy, C. Louis, K. Hadjiivanov, J. Mater. Sci. 42 (2007) 3299.
[31] M.Y. Mihaylov, J.C. Fierro-Gonzalez, H. Knoezinger, B.C. Gates, K.I. Hadjiivanov, J. Phys. Chem. B 110 (2006) 7695.
[32] M. Mihaylov, B.C. Gates, J.C. Fierro-Gonzalez, K. Hadjiivanov, H. Knozinger, J. Phys. Chem. C 111 (2007) 2548.
[33] D. Tibiletti, A. Amieiro-Fonseca, R. Burch, Y. Chen, J.M. Fisher, A. Goguet, C. Hardacre, P. Hu, D. Thompsett, J. Phys. Chem. B 109 (2005) 22553.
[34] X. Wang, J.A. Rodriguez, J.C. Hanson, M. Perez, J. Evans, J. Chem. Phys. 123 (2005) 221101.
[35] S. Ricote, G. Jacobs, M. Milling, Y. Ji, P.M. Patterson, B.H. Davis, Appl. Catal. A 303 (2006) 35.
[36] F.C. Meunier, D. Tibiletti, A. Goguet, D. Reid, R. Burch, Appl. Catal. A 289 (2005) 104.
[37] D. Tibiletti, A. Goguet, D. Reid, F.C. Meunier, R. Burch, Catal. Today 113 (2006) 94.
[38] C. Binet, M. Daturi, J.C. Lavalley, Catal. Today 50 (1999) 207.
[39] M. Daturi, E. Finocchio, C. Binet, J.C. Lavalley, F. Fally, V. Perrichon, J. Phys. Chem. B 103 (1999) 4884.
[40] C. Binet, A. Badri, J.-C. Lavalley, J. Phys. Chem. 98 (1994) 6392.
[41] C. Fontaine-Gautrelet, J.-M. Krafft, G. Djega-Mariadassou, C. Thomas, J. Catal. 247 (2007) 34.
[42] F.C. Meunier, D. Reid, A. Goguet, S. Shekhtman, C. Hardacre, R. Burch, W. Deng, M. Flytzani-Stephanopoulos, J. Catal. 247 (2007) 277.
[43] A. Karpenko, R. Leppelt, V.A. Plzak, R.J. Behm, J. Catal. 252 (2007) 231.
[44] S.L. Shannon, J.G. Goodwin, Chem. Rev. 95 (1995) 677.
[45] A. Goguet, D. Tibiletti, F.C. Meunier, J.P. Breen, R. Burch, J. Phys. Chem. B 108 (2004) 20240.
[46] Y. Yang, R.S. Disselkamp, J. Szanyi, C.H.F. Peden, C.T. Campbell, J.G. Goodwin, Rev. Sci. Inst. 77 (2006) 094104.

[47] C.N. Costa, A.M. Efstathiou, J. Phys. Chem. C 111 (2007) 3010.
[48] M.W. Balakos, S.S.C. Chuang, G. Srivinas, J. Catal. 140 (1993) 281.
[49] F.C. Meunier, A. Goguet, C. Hardacre, R. Burch, D. Thompsett, J. Catal. 252 (2007) 18.
[50] D. Tibiletti, F.C. Meunier, A. Goguet, D. Reid, R. Burch, M. Boaro, M. Vicario, A. Trovarelli, J. Catal. 244 (2006) 183.
[51] F.C. Meunier, D. Tibiletti, A. Goguet, S. Shekhtman, C. Hardacre, R. Burch, Catal. Today 126 (2007) 143.
[52] A. Goguet, R. Burch, Y. Chen, C. Hardacre, P. Hu, R.W. Joyner, F.C. Meunier, B.S. Mun, D. Thompsett, D. Tibiletti, J. Phys. Chem. C 111 (2007) 16927.
[53] J. Sirita, S. Phanichphant, F.C. Meunier, Anal. Chem. 79 (2007) 3912.
[54] A.M. O`Connor, F.C. Meunier, J.R.H. Ross, Stud. Surf. Sci. Catal. 119 (1998) 819.
[55] B. Yoon, H. Hakkinen, U. Landman, A.S. Worz, J.M. Antonietti, S. Abbet, K. Judai, U. Heiz, Science 307 (2005) 403.